

Guodong Liu

State Key Laboratory of Nonlinear Mechanics,
Institute of Mechanics,
Chinese Academy of Sciences,
Beijing 100190, China;
School of Engineering Science,
University of Chinese Academy of Sciences,
Beijing 100049, China
e-mail: liuguodong@imech.ac.cn

Lijuan Sun

State Key Laboratory of Nonlinear Mechanics,
Institute of Mechanics,
Chinese Academy of Sciences,
Beijing 100190, China;
School of Engineering Science,
University of Chinese Academy of Sciences,
Beijing 100049, China
e-mail: sunlj@lnm.imech.ac.cn

Yewang Su¹

State Key Laboratory of Nonlinear Mechanics,
Institute of Mechanics,
Chinese Academy of Sciences,
Beijing 100190, China;
School of Engineering Science,
University of Chinese Academy of Sciences,
Beijing 100049, China;
State Key Laboratory of Structural Analysis for
Industrial Equipment,
Department of Engineering Mechanics,
Dalian University of Technology,
Dalian 116024, China
e-mail: yewangsu@imech.ac.cn

Scaling Effects in the Mechanical System of the Flexible Epidermal Electronics and the Human Skin

The “island-bridge” mesh structure is widely adopted for flexible epidermal electronics to simultaneously achieve the electronic functions and mechanical flexibility. Mechanical intuition tells that the small size of the “island” is beneficial to the flexibility of the structure and the adaptability to complex geometric targets. Here, a plane-strain model and an axisymmetric model are established for square “island” and cycle “island,” respectively, to analyze the mechanical system consisting of the flexible epidermal electronics and the human skin. It is found that the pressure between the “island” and the human skin is positive at the inner region and reaches a peak value at the center, while is negative at the outer region and approaches infinite at the boundary of the contact region. With the increase in the size a/R_0 , the amplitude of the pressure significantly increases, as well as the singular degree of the pressure at the boundary. The reduction of the “island” size is beneficial for the optimization of the “comfort level” of the flexible epidermal electronics. The models degenerate into the famous Johnson-Kendall-Roberts (JKR) model for the limit case with extremely hard and thick “island.” [DOI: 10.1115/1.4047039]

Keywords: flexible electronics, epidermal electronics, size effect, JKR model, elasticity, structures

1 Introduction

Flexible epidermal electronics, integrating electronic circuits, and functional components, such as sensors and actuators [1], have been extensively developed in recent years due to the widely applications to the healthcare monitoring [2–6], the human-machine interaction interfaces [7–10], motion capture [10–14], remote communications [8,15], and physical therapy [16,17]. With the advanced mechanical structures and materials, flexible epidermal electronics are capable of being stretched, bent, and twisted without damage, as shown in Fig. 1(a) [1,8,10,16]. The “island-bridge” mesh structure consisting of “islands” and “bridges” is the most popular structure to simultaneously achieve the electronic functions and the mechanical flexibility (Figs. 1(b) and 1(c) [10,18]). The “islands” integrating functional components undergo less deform during the deformation of the flexible epidermal electronics, while the “bridges” provide both deformability and the electronic conductivity [18,19]. Some progress has been made in the studies on mechanics of the flexible epidermal electronics [20,21]. From the view of mechanics, the small size of the “island” is beneficial to the flexibility of the structure and the adaptability to complex geometric targets. However, the size of the “island” is limited in many practical cases probably because of the fabrication techniques, the size of the functional components, the commercial cost, etc. On the other hand, the large size of the “island” of the flexible epidermal electronics may yield the excessive constraint or deformation for the human

skin. How small should the size of the “islands” be and what principles should the size design follow?

The objective of this work is to establish analytic models to analyze the mechanical system consisting of the flexible epidermal electronics and the human skin. For square “island” [18] and cycle “island” [10], a plane-strain model and an axisymmetric model are established in Secs. 2 and 3, respectively. The size effects on the interactional pressure between the “island” and the human skin are systematically studied. Concluding remarks are given in Sec. 4.

2 The Plane-Strain Model

An “island-bridge” mesh structure bonded on a cylinder human tissue with skin is illustrated in Fig. 2(a). For the analysis of the interaction between the “island” and human skin, a plane-strain model is established as shown in Fig. 2(b). The “island” integrated with hard functional components is modeled as an elastic beam with the width of $2a$, thickness of t , Young’s modulus E_{island} and Poisson’s ratio ν_{island} , respectively. The human tissue and skin are simplified as a linear elastic circle, with radius R_0 , Young’s modulus E_{skin} and Poisson’s ratio ν_{skin} . Before bonding together, they contact each other at the center of the bottom surface of the “island,” where the origin of the coordinate is located. With pressure and adhesive, the flexible epidermal electronics is bonded on the skin. The contact areas between the “island” and the skin become $2a$. It is rather complicated to strictly solve this problem of contact mechanics, because it involves an integral equation coupling single integral term and double integral term. In this model, the elastic circle for skin is deal with the Herz theory of contact

¹Corresponding author.

Contributed by the Applied Mechanics Division of ASME for publication in the JOURNAL OF APPLIED MECHANICS. Manuscript received March 15, 2020; final manuscript received April 15, 2020; published online May 29, 2020. Assoc. Editor: Yong Zhu.

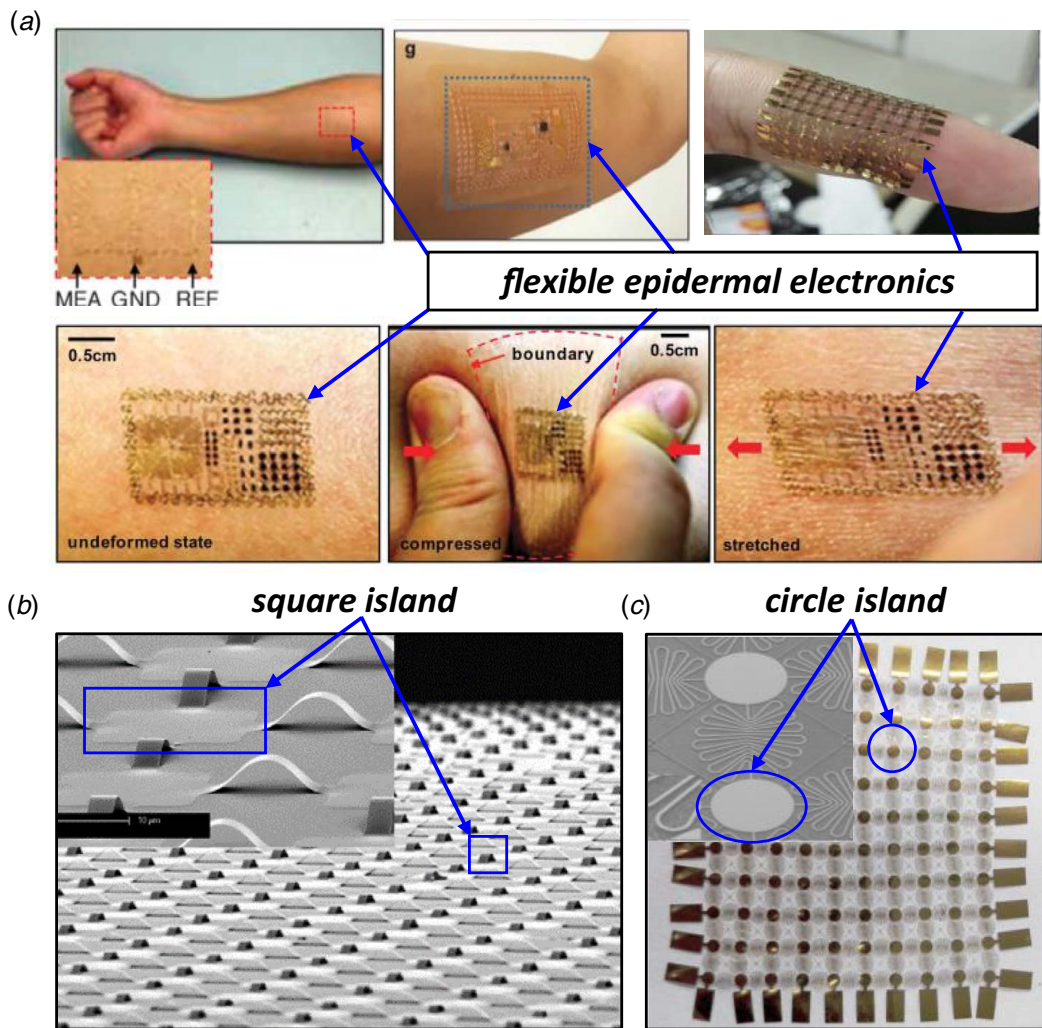


Fig. 1 (a) Flexible epidermal electronics [1,8,10,16] mounted on the human skin. Scanning electron microscopic images of the classical “island-bridge” structure with (b) square “island” [18] and (c) circle “island” [10]. (Reproduced with permission from The American Association for the Advancement of Science © 2011 [1], John Wiley and Sons © 2013 [8], John Wiley and Sons © 2020 [16], and Springer Nature @ 2008 [18]).

mechanics [22], while energy method will be applied to couple the deformation of the two elastic bodies.

Let x and z be the coordinates of the horizontal axis and vertical axis, respectively. The mechanical analysis of the elastic circle is based on the following hypotheses: (1) the contact size is much smaller than the radius of the human tissue and skin, i.e., $2a \ll R_0$; (2) the friction along the x direction at the interface is neglected. According to the Herz theory of contact mechanics [22], the pressure distribution at the interface can be obtained as

$$p(x) = p_1 \left(1 - \frac{x^2}{a^2}\right)^{-\frac{1}{2}} + p_2 \left(1 - \frac{x^2}{a^2}\right)^{\frac{1}{2}} \quad (1)$$

where p_1 and p_2 are constants to be determined. The corresponding displacement [22] of the surface of the human skin is

$$w_{\text{skin}}(x) = \frac{p_2(1 - \nu_{\text{skin}}^2)}{aE_{\text{skin}}} x^2 \quad (2)$$

Here, the term of the constant displacement yielded by $p_1(1 - x^2/a^2)^{-1/2}$ and $p_2(1 - x^2/a^2)^{1/2}$ in Eq. (1) vanishes because of the condition of $w_{\text{skin}}(x=0) = 0$. The condition of traction free on the top of the “island” requires that the resultant force is zero, i.e.,

$$\int_{-a}^a p(x) dx = 0 \quad (3)$$

The deformation of the human skin couples with that of the “island.” The geometric analysis yields the condition

$$w_{\text{skin}}(x) = \frac{x^2}{2R_0} - \frac{x^2}{2R_1} \quad (4)$$

Here, R_1 is the radius of the interface after the deformation, which is a constant to be determined. Substitution of Eqs. (1) and (2) into Eqs. (3) and (4) determines the constants p_1 and p_2 as

$$p_1 = -\frac{aE_{\text{skin}}}{4(1 - \nu_{\text{skin}}^2)} \left(\frac{1}{R_0} - \frac{1}{R_1}\right), \quad p_2 = \frac{aE_{\text{skin}}}{2(1 - \nu_{\text{skin}}^2)} \left(\frac{1}{R_0} - \frac{1}{R_1}\right) \quad (5)$$

The pressure distribution $p(x)$ can be subsequently obtained as

$$p(x) = \frac{aE_{\text{skin}}}{4(1 - \nu_{\text{skin}}^2)} \left(\frac{1}{R_0} - \frac{1}{R_1}\right) \left[2 \left(1 - \frac{x^2}{a^2}\right)^{\frac{1}{2}} - \left(1 - \frac{x^2}{a^2}\right)^{-\frac{1}{2}} \right] \quad (6)$$

For the deformation of the “island,” the displacement is assumed as a quadratic function in harmony with the deformation of the human skin, given by

$$w_{\text{island}}(x) = -\frac{x^2}{2R_1} \quad (7)$$

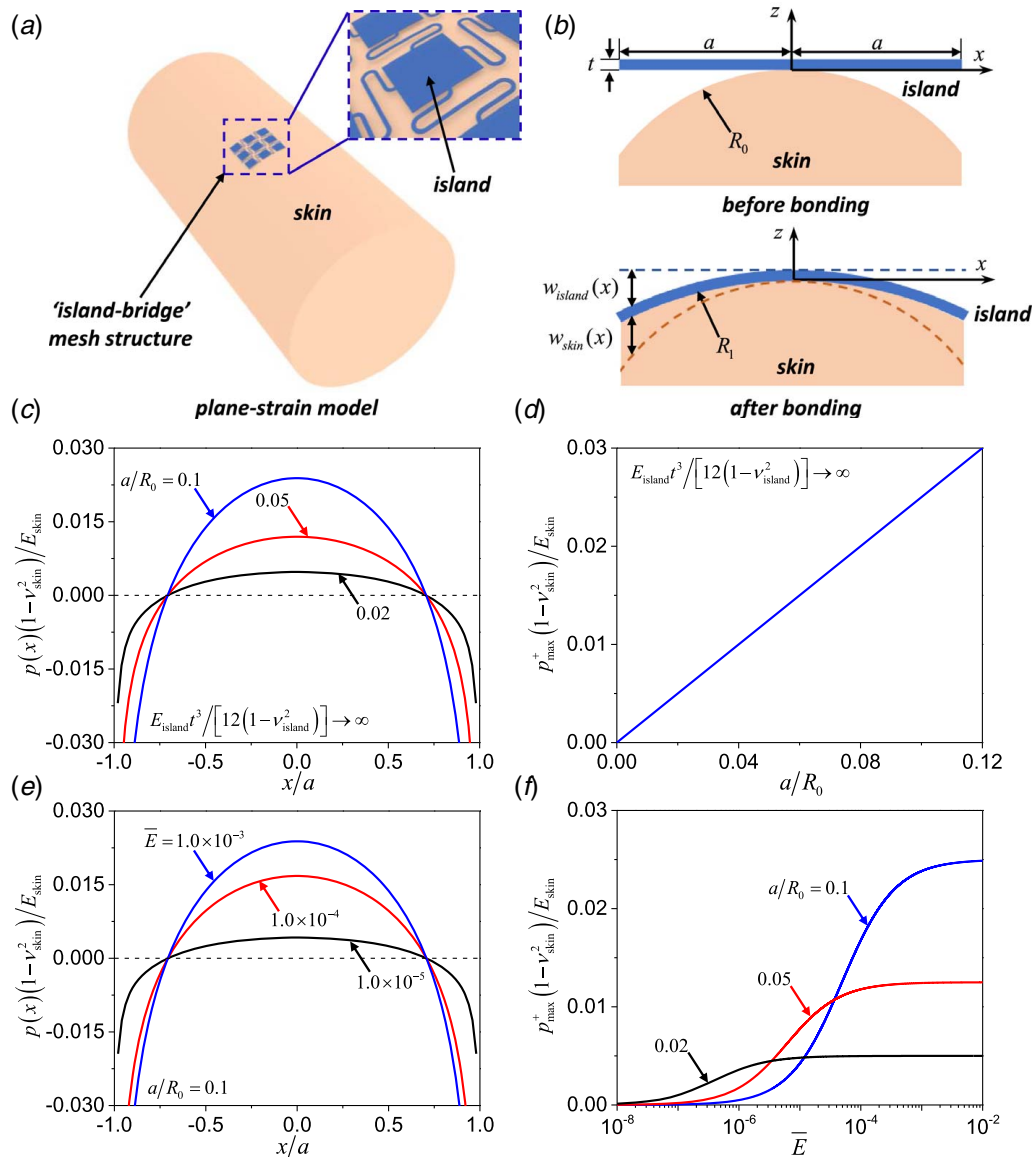


Fig. 2 (a) Schematic illustration of the “island-bridge” mesh structure bonded on an elastic cylinder. (b) Schematic illustration for the plane-strain model with the regimes before and after bonding. (c) The distribution of the dimensionless pressure $p(x)(1-\nu_{skin}^2)/E_{skin}$ and (d) the size effect on the peak of the positive dimensionless pressure $p_{max}^+(1-\nu_{skin}^2)/E_{skin}$, for $E_{island}t^3/[12(1-\nu_{island}^2)] \rightarrow \infty$. (e) Effects of the dimensionless bending stiffness \bar{E} on the distribution of the dimensionless pressure $p(x)(1-\nu_{skin}^2)/E_{skin}$, for $a/R_0 = 0.1$. (f) Curves of the peak of the positive dimensionless pressure $p_{max}^+(1-\nu_{skin}^2)/E_{skin}$ versus the bending stiffness \bar{E} , for $a/R_0 = 0.1, 0.05, 0.02$.

Here, the energy method is used to determine the radius R_1 . The theory of beams gives the elastic energy of the “island” as

$$U_{island} = \int_{-a}^a \frac{1}{2} \frac{E_{island}t^3}{12(1-\nu_{island}^2)} \left[\frac{d^2 w_{island}(x)}{dx^2} \right]^2 dx \quad (8)$$

where $E_{island}t^3/[12(1-\nu_{island}^2)]$ is the bending stiffness of the “island.” The elastic energy of the human skin can be obtained by the work of the pressure on the surface displacement, given by

$$U_{skin} = \int_{-a}^a \frac{1}{2} [-p(x)]w_{skin}(x)dx \quad (9)$$

Here, “-” means the defined directions of $p(x)$ and $w_{skin}(x)$ are the opposite. The optimization of the total energy of the

system requires

$$\frac{\partial}{\partial R_1} (U_{island} + U_{skin}) = 0 \quad (10)$$

Substitution of Eqs. (2) and (6–9) into Eq. (10) yields

$$R_1 = \left[1 + \frac{16E_{island}t^3(1-\nu_{skin}^2)}{3\pi a^3 E_{skin}(1-\nu_{island}^2)} \right] R_0 \quad (11)$$

which, together with Eq. (6), results in the final pressure distribution as

$$p(x) = - \frac{4aE_{skin}E_{island}t^3}{16R_0E_{island}t^3(1-\nu_{skin}^2) + 3\pi R_0a^3E_{skin}(1-\nu_{island}^2)} \times \left[2 \left(1 - \frac{x^2}{a^2} \right)^{\frac{1}{2}} - \left(1 - \frac{x^2}{a^2} \right)^{-\frac{1}{2}} \right] \quad (12)$$

For very thin and soft “island,” $E_{\text{island}}t^3/[12(1-\nu_{\text{island}}^2)] \rightarrow 0$. The deformation of the human skin and pressure vanish. For the thick and hard “island,” $E_{\text{island}}t^3/[12(1-\nu_{\text{island}}^2)] \rightarrow \infty$. Equation (12) degenerates to

$$p(x) = \frac{aE_{\text{skin}}}{4R_0(1-\nu_{\text{skin}}^2)} \left[2\left(1 - \frac{x^2}{a^2}\right)^{\frac{1}{2}} - \left(1 - \frac{x^2}{a^2}\right)^{-\frac{1}{2}} \right] \quad (13)$$

which is actually the famous Johnson-Kendall-Roberts (JKR) model [22].

For simplicity, the case with rigid “island” ($E_{\text{island}}t^3/[12(1-\nu_{\text{island}}^2)] \rightarrow \infty$) is analyzed first. The distribution of the dimensionless pressure $p(x)(1-\nu_{\text{skin}}^2)/E_{\text{skin}}$ is plotted in Fig. 2(c). The pressure is positive at the inner region and reaches a peak value at the center, while is negative at the outer region and approaches infinite at the boundary of the contact region. The effects of the size a/R_0 on the pressure distribution and amplitude are also studied as shown in Fig. 2(c). With the increase in the size a/R_0 , the amplitude of the pressure significantly increases, as well as the singular degree of the pressure at the boundary. Particularly, the peak of the positive dimensionless pressure $p_{\text{max}}^+(1-\nu_{\text{skin}}^2)/E_{\text{skin}}$ is defined to quantitatively present the stress/strain magnitude in the human skin, while the negative pressure is singular at the boundary. As shown in Figs. 2(c) and 2(d), the peak of the positive dimensionless pressure increases from 0.00025 to 0.025, when the size a/R_0 increases from 0.001 to 0.1. It means that the large size of the “island” results large positive or negative pressure on the skin, which may yields the uncomfortable feeling for human. The reduction in the “island” size is beneficial for the optimization of the “comfort level” of the flexible epidermal electronics.

Effects of the dimensionless bending stiffness $\bar{E} = \{E_{\text{island}}t^3/[12(1-\nu_{\text{island}}^2)]\}/[E_{\text{skin}}R_0^3/(1-\nu_{\text{skin}}^2)]$ on the distribution of the dimensionless pressure $p(x)(1-\nu_{\text{skin}}^2)/E_{\text{skin}}$ are also shown in Fig. 2(e). For $a/R_0 = 0.1$, the amplitude of the pressure increases with the increase in the bending stiffness, as well as the singular degree of the pressure at the boundary. Figure 2(f) gives the curves of the peak of the positive dimensionless pressure versus the bending stiffness. For $a/R_0 = 0.1$, the peak of the positive dimensionless pressure increases from 0.004 to 0.017, when the dimensionless bending stiffness increases from 1×10^{-5} to 1×10^{-4} . As an example, the optimized design of a flexible epidermal electronic [23] with the width $2a = 0.2$ mm, thickness $t = 0.5$ μm , Young’s modulus $E_{\text{island}} = 200$ GPa, Poisson’s ratio $\nu_{\text{island}} = 0.3$, the radius of the forehead $R_0 \approx 0.5$ m [24], Young’s modulus $E_{\text{skin}} = 150$ kPa, and Poisson’s ratio $\nu_{\text{skin}} = 0.495$ yields a peak of the positive dimensionless pressure $p_{\text{max}}^+(1-\nu_{\text{skin}}^2)/E_{\text{skin}} = 1 \times 10^{-5}$, which is very small to sense for human skin.

3 The Axisymmetric Model

Similarly, the aforementioned analysis can be extended to an axisymmetric model. An “island-bridge” mesh structure bonded on a sphere human tissue with skin is illustrated in Fig. 3(a). In the analysis, the “island” is modeled as a circular plane, while the human tissue and skin becomes an elastic sphere. Figure 3(b) shows the axisymmetric mechanical model for the interaction between the “island” and the human skin. The above hypotheses hold here for the axisymmetric analysis. Herz theory of contact mechanics [22], together with the conditions of zero resultant force and the geometric analysis, yields the pressure distribution at the interface as

$$p(r) = \frac{2aE_{\text{skin}}}{3\pi(1-\nu_{\text{skin}}^2)} \left(\frac{1}{R_0} - \frac{1}{R_1} \right) \left[3\left(1 - \frac{r^2}{a^2}\right)^{\frac{1}{2}} - \left(1 - \frac{r^2}{a^2}\right)^{-\frac{1}{2}} \right] \quad (14)$$

and the displacement of the surface of the human skin as

$$w_{\text{skin}}(r) = \frac{r^2}{2R_0} - \frac{r^2}{2R_1} \quad (15)$$

Here, R_1 is the radius of the interface after the deformation, which is a constant to be determined. The energy method is also adapted to determine the radius R_1 . The theory of plates gives the elastic energy of the “island” as

$$U_{\text{island}} = \int_0^{2\pi} \int_0^a \frac{1}{2} \frac{E_{\text{island}}t^3}{12(1-\nu_{\text{island}}^2)} \left\{ r \left[\frac{d^2w_{\text{island}}(r)}{dr^2} \right]^2 + \frac{1}{r} \left[\frac{dw_{\text{island}}(r)}{dr} \right]^2 \right\} r dr d\theta + 2\nu_{\text{island}} \frac{dw_{\text{island}}(r)}{dr} \frac{d^2w_{\text{island}}(r)}{dr^2} \quad (16)$$

where $E_{\text{island}}t^3/[12(1-\nu_{\text{island}}^2)]$ is the bending stiffness of the “island”

$$w_{\text{island}}(r) = -\frac{r^2}{2R_1} \quad (17)$$

is the displacement of the island in harmony with the deformation of the human skin. The elastic energy of the human skin can be obtained by the work of the pressure on the surface displacement, given by

$$U_{\text{skin}} = \int_0^{2\pi} \int_0^a \frac{1}{2} [-p(r)]w_{\text{skin}}(r)r dr d\theta \quad (18)$$

The optimization of the total energy of the system $\partial(U_{\text{island}} + U_{\text{skin}})/\partial R_1 = 0$ gives the radius $R_1 = \{1 + 15\pi E_{\text{island}}t^3(1-\nu_{\text{skin}}^2)/[16a^3E_{\text{skin}}(1-\nu_{\text{island}})]\}R_0$, which, together with Eq. (14), results the pressure distribution as

$$p(r) = \frac{10aE_{\text{skin}}E_{\text{island}}t^3}{15\pi R_0 E_{\text{island}}t^3(1-\nu_{\text{skin}}^2) + 16R_0 a^3 E_{\text{skin}}(1-\nu_{\text{island}})} \times \left[3\left(1 - \frac{r^2}{a^2}\right)^{\frac{1}{2}} - \left(1 - \frac{r^2}{a^2}\right)^{-\frac{1}{2}} \right] \quad (19)$$

For very thin and soft “island,” $E_{\text{island}}t^3/(1-\nu_{\text{island}}) \rightarrow 0$. The deformation of the human skin and the pressure vanish. For the thick and hard “island,” $E_{\text{island}}t^3/(1-\nu_{\text{island}}) \rightarrow \infty$. Equation (19) degenerates to

$$p(r) = \frac{2aE_{\text{skin}}}{3\pi R_0(1-\nu_{\text{skin}}^2)} \left[3\left(1 - \frac{r^2}{a^2}\right)^{\frac{1}{2}} - \left(1 - \frac{r^2}{a^2}\right)^{-\frac{1}{2}} \right] \quad (20)$$

which is the axisymmetric JKR model [22].

The numerical results are similar to that for the plane-strain model. In the case of $E_{\text{island}}t^3/(1-\nu_{\text{island}}) \rightarrow \infty$, the pressure is positive at the inner region and reaches a peak value at the center, while is negative at the outer region and approaches infinite at the boundary (Fig. 3(c)). As shown in Fig. 3(d), with the increase in the size a/R_0 from 0.001 to 0.1, the peak of the positive dimensionless pressure $p_{\text{max}}^+(1-\nu_{\text{skin}}^2)/E_{\text{skin}}$ increases from 0.0004 to 0.0424, which means that the large size of the “island” results large positive or negative pressure on the skin and may yield the uncomfortable feeling for human. Furthermore, Fig. 3(f) shows the effects of the dimensionless bending stiffness $\bar{D} = \{E_{\text{island}}t^3/(1-\nu_{\text{island}})\}/[E_{\text{skin}}R_0^3/(1-\nu_{\text{skin}}^2)]$ on the distribution of the dimensionless pressure $p(r)(1-\nu_{\text{skin}}^2)/E_{\text{skin}}$ for $a/R_0 = 0.1$. With the increase in the bending stiffness, the amplitude of the pressure increases, as well as the singular degree of the pressure at the boundary of the contact region. The relationships between the positive dimensionless pressure and the dimensionless bending stiffness are also studied in Fig. 3(f). For $a/R_0 = 0.1$, the peak of the positive dimensionless pressure increases from 0.0097 to 0.0317, when the dimensionless bending stiffness increases from 1×10^{-4} to 1×10^{-3} .

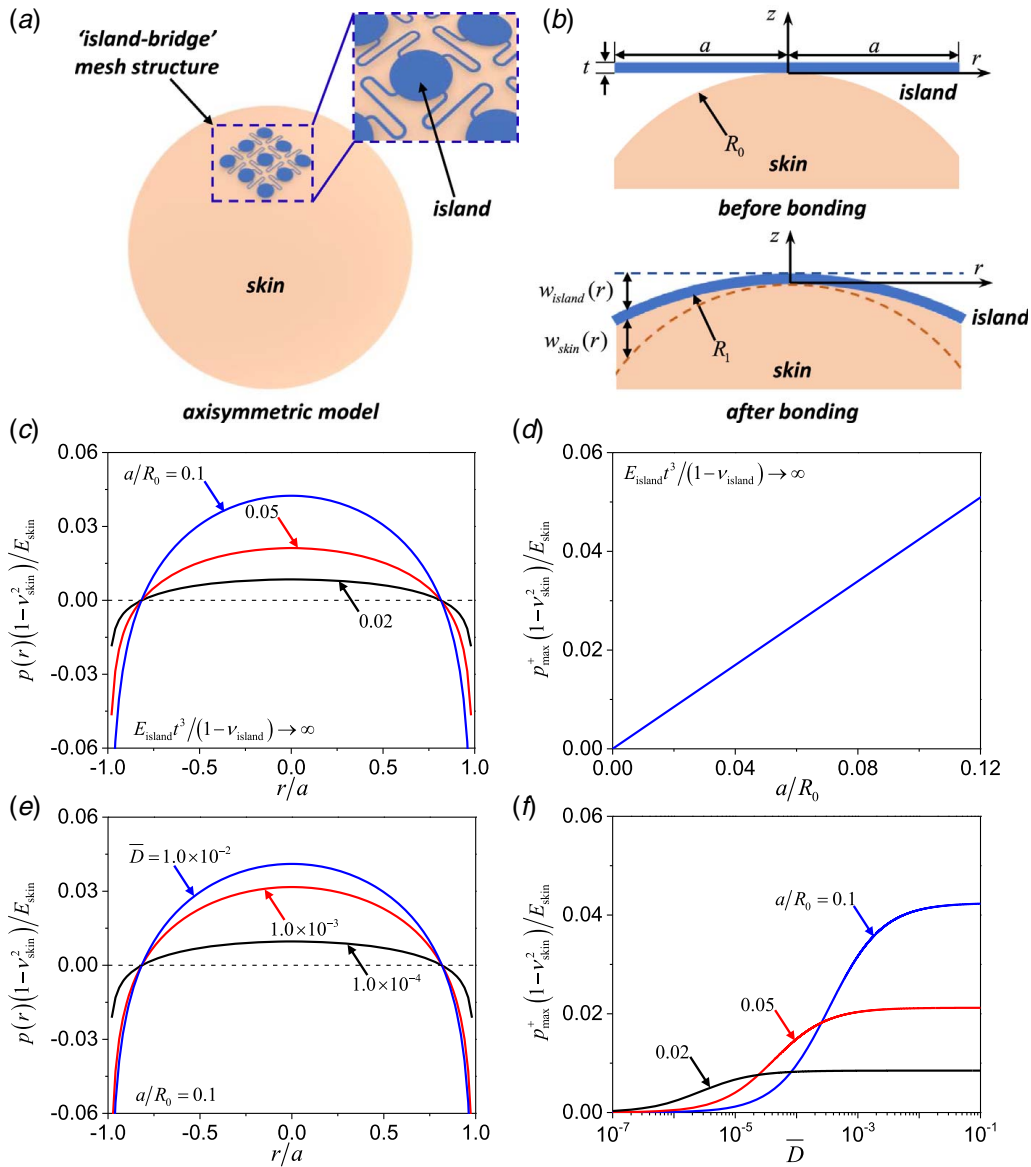


Fig. 3 (a) Schematic illustration of the “island-bridge” mesh structure bonded on an elastic sphere. (b) Schematic illustration for the axisymmetric model with the regimes before and after bonding. (c) The distribution of the dimensionless pressure $p(r)(1-\nu_{skin}^2)/E_{skin}$ and (d) the size effect on the peak of the positive dimensionless pressure $p_{max}^+(1-\nu_{skin}^2)/E_{skin}$, for $E_{island}t^3/(1-\nu_{island}) \rightarrow \infty$. (e) Effects of the dimensionless bending stiffness \bar{D} on the distribution of the dimensionless pressure $p(r)(1-\nu_{skin}^2)/E_{skin}$, for $a/R_0 = 0.1$. (f) Curves of the peak of the positive dimensionless pressure $p_{max}^+(1-\nu_{skin}^2)/E_{skin}$ versus the bending stiffness \bar{D} , for $a/R_0 = 0.1, 0.05, 0.02$.

4 Concluding Remarks

- (1) For square “island” and cycle “island,” a plane-strain model and an axisymmetric model have been established to analyze the mechanical system consisting of the flexible epidermal electronics and the human skin, respectively.
- (2) It is found that the pressure between the “island” and the human skin is positive at the inner region and reaches a peak value at the center, while is negative at the outer region and approaches infinite at the boundary of the contact region.
- (3) With the increase in the size a/R_0 , the amplitude of the pressure significantly increases, as well as the singular degree of the pressure at the boundary. The reduction of the “island” size is beneficial for the optimization of the “comfort level” of the flexible epidermal electronics.

- (4) The models degenerate into the famous JKR model for the limit case with extremely hard and thick “island.”
- (5) The aforementioned analysis and results are universal for the “island” of flexible epidermal electronics consisting of multilayer structures with different materials, when the bending stiffness and the Poisson’s ratio of the “island” are replaced by the effective bending stiffness and the effective Poisson’s ratio of the multilayer “island”, respectively.
- (6) Conclusions (2), (3), and (5) hold for other “islands” with arbitrary shapes.

Acknowledgment

Y.S. gratefully acknowledges the support from the National Natural Science Foundation of China (Grants Nos. 11772331 and 11572323), Beijing Municipal Science and Technology Commission (Z191100002019010), Beijing Municipal Natural Science

Foundation (Grant No. 2202066), Key Research Program of Frontier Sciences of the Chinese Academy of Sciences (ZDBS-LY-JSC014), Chinese Academy of Sciences via the “Hundred Talent Program”, Strategic Priority Research Program of the Chinese Academy of Sciences (No. XDB22040501), Beijing Institute of Space Mechanics & Electricity, and the State Key Laboratory of Structural Analysis for Industrial Equipment, Dalian University of Technology (Grant No. GZ19102). G. L., L. S. and Y. S. conceived the concept, conducted the theoretical derivation, analyzed all the data and prepared the manuscript. Y. S. supervised the project.

Competing Interests

The authors declare no competing interests.

References

- [1] Kim, D. H., Lu, N. S., Ma, R., Kim, Y. S., Kim, R. H., Wang, S. D., Wu, J., Won, S. M., Tao, H., Islam, A., Yu, K. J., Kim, T. I., Chowdhury, R., Ying, M., Xu, L. Z., Li, M., Chung, H. J., Keum, H., McCormick, M., Liu, P., Zhang, Y. W., Omenetto, F. G., Huang, Y. G., Coleman, T., and Rogers, J. A., 2011, “Epidermal Electronics,” *Science*, **333**(6044), pp. 838–843.
- [2] Jayathilaka, W., Qi, K., Qin, Y. L., Chinnappan, A., Serrano-Garcia, W., Baskar, C., Wang, H. B., He, J. X., Cui, S. Z., Thomas, S. W., and Ramakrishna, S., 2019, “Significance of Nanomaterials in Wearables: A Review on Wearable Actuators and Sensors,” *Adv. Mater.*, **31**(7), p. 1805921.
- [3] Yokota, T., Zalar, P., Kaltenbrunner, M., Jinno, H., Matsuhisa, N., Kitanosako, H., Tachibana, Y., Yukita, W., Koizumi, M., and Someya, T., 2016, “Ultraflexible Organic Photonic Skin,” *Sci. Adv.*, **2**(4), p. e1501856.
- [4] Das, P. S., Park, S. H., Baik, K. Y., Lee, J. W., and Park, J. Y., 2020, “Thermally Reduced Graphene Oxide-Nylon Membrane Based Epidermal Sensor Using Vacuum Filtration for Wearable Electrophysiological Signals and Human Motion Monitoring,” *Carbon*, **158**(1), pp. 386–393.
- [5] Reeder, J. T., Choi, J., Xue, Y. G., Gutruf, P., Hanson, J., Liu, M., Ray, T., Bandothkar, A. J., Avila, R., Xia, W., Krishnan, S., Xu, S., Barnes, K., Pahnke, M., Ghaffari, R., Huang, Y., and Rogers, J. A., 2019, “Waterproof, Electronics-Enabled, Epidermal Microfluidic Devices for Sweat Collection, Biomarker Analysis, and Thermography in Aquatic Settings,” *Sci. Adv.*, **5**(1), p. eaau6356.
- [6] Xu, S., Zhang, Y. H., Jia, L., Mathewson, K. E., Jang, K. I., Kim, J., Fu, H. R., Huang, X., Chava, P., Wang, R. H., Bhole, S., Wang, L. Z., Na, Y. J., Guan, Y., Flavin, M., Han, Z. S., Huang, Y. G., and Rogers, J. A., 2014, “Soft Microfluidic Assemblies of Sensors, Circuits, and Radios for the Skin,” *Science*, **344**(6179), pp. 70–74.
- [7] Imani, S., Bandothkar, A. J., Mohan, A. M. V., Kumar, R., Yu, S. F., Wang, J., and Mercier, P. P., 2016, “A Wearable Chemical-Electrophysiological Hybrid Biosensing System for Real-Time Health and Fitness Monitoring,” *Nat. Commun.*, **7**(1), p. 11650.
- [8] Jeong, J. W., Yeo, W. H., Akhtar, A., Norton, J. J. S., Kwack, Y. J., Li, S., Jung, S. Y., Su, Y. W., Lee, W., Xia, J., Cheng, H. Y., Huang, Y. G., Choi, W. S., Bretl, T., and Rogers, J. A., 2013, “Materials and Optimized Designs for Human-Machine Interfaces via Epidermal Electronics,” *Adv. Mater.*, **25**(47), pp. 6839–6846.
- [9] Liu, Y. H., Norton, J. J. S., Qazi, R., Zou, Z. N., Ammann, K. R., Liu, H., Yan, L. Q., Tran, P. L., Jang, K. I., Lee, J. W., Zhang, D., Kilian, K. A., Jung, S. H., Bretl, T., Xiao, J. L., Slepian, M. J., Huang, Y. G., Jeong, J. W., and Rogers, J. A., 2016, “Epidermal Mechano-Acoustic Sensing Electronics for Cardiovascular Diagnostics and Human-Machine Interfaces,” *Sci. Adv.*, **2**(11), p. e1601185.
- [10] Hua, Q. L., Sun, J. L., Liu, H. T., Bao, R. R., Yu, R. M., Zhai, J. Y., Pan, C. F., and Wang, Z. L., 2018, “Skin-Inspired Highly Stretchable and Conformable Matrix Networks for Multifunctional Sensing,” *Nat. Commun.*, **9**(1), p. 244.
- [11] Lai, Y. C., Wu, H. M., Lin, H. C., Chang, C. L., Chou, H. H., Hsiao, Y. C., and Wu, Y. C., 2019, “Entirely, Intrinsically, and Autonomously Self-Healable, Highly Transparent, and Superstretchable Triboelectric Nanogenerator for Personal Power Sources and Self-Powered Electronic Skins,” *Adv. Funct. Mater.*, **29**(40), p. 1904626.
- [12] Song, Y., Chen, H. T., Su, Z. M., Chen, X. X., Miao, L. M., Zhang, J. X., Cheng, X. L., and Zhang, H. X., 2017, “Highly Compressible Integrated Supercapacitor-Piezoresistance-Sensor System With CNT-PDMS Sponge for Health Monitoring,” *Small*, **13**(39), p. 1702091.
- [13] Ryu, S., Lee, P., Chou, J. B., Xu, R. Z., Zhao, R., Hart, A. J., and Kim, S. G., 2015, “Extremely Elastic Wearable Carbon Nanotube Fiber Strain Sensor for Monitoring of Human Motion,” *ACS Nano*, **9**(6), pp. 5929–5936.
- [14] Lipomi, D. J., Vosgueritchian, M., Tee, B. C., Hellstrom, S. L., Lee, J. A., Fox, C. H., and Bao, Z. J. N. n., 2011, “Skin-Like Pressure and Strain Sensors Based on Transparent Elastic Films of Carbon Nanotubes,” *Nat. Nanotechnol.*, **6**(12), pp. 788–792.
- [15] Hou, C., Xu, Z. J., Qiu, W., Wu, R. H., Wang, Y. N., Xu, Q. C., Liu, X. Y., and Guo, W. X., 2019, “A Biodegradable and Stretchable Protein-Based Sensor as Artificial Electronic Skin for Human Motion Detection,” *Small*, **15**(11), p. 1805084.
- [16] Jeong, H., Wang, L., Ha, T., Mitbender, R., Yang, X. X., Dai, Z. H., Qiao, S. T., Shen, L. X., Sun, N., and Lu, N. S., 2019, “Modular and Reconfigurable Wireless E-Tattoos for Personalized Sensing,” *Adv. Mater. Technol.*, **4**(8), p. 1900117.
- [17] Son, D., Lee, J., Qiao, S., Ghaffari, R., Kim, J., Lee, J. E., Song, C., Kim, S. J., Lee, D. J., Jun, S. W., Yang, S., Park, M., Shin, J., Do, K., Lee, M., Kang, K., Hwang, C. S., Lu, N., Hyeon, T., and Kim, D.-H., 2014, “Multifunctional Wearable Devices for Diagnosis and Therapy of Movement Disorders,” *Nat. Nanotechnol.*, **9**(5), pp. 397–404.
- [18] Ko, H. C., Stoykovich, M. P., Song, J., Malyarchuk, V., Choi, W. M., Yu, C.-J., Geddes, I. J., Xiao, J., Wang, S., and Huang, Y. J. N., 2008, “A Hemispherical Electronic eye Camera Based on Compressible Silicon Optoelectronics,” *Nature*, **454**(7205), pp. 748–753.
- [19] Li, R., Li, M., Su, Y., Song, J., and Ni, X., 2013, “An Analytical Mechanics Model for the Island-Bridge Structure of Stretchable Electronics,” *Soft Matter*, **9**(35), pp. 8476–8482.
- [20] Wang, S. D., Li, M., Wu, J., Kim, D. H., Lu, N. S., Su, Y. W., Kang, Z., Huang, Y. G., and Rogers, J. A., 2012, “Mechanics of Epidermal Electronics,” *ASME J. Appl. Mech.*, **79**(3), p. 031022.
- [21] Cheng, H., and Wang, S., 2014, “Mechanics of Interfacial Delamination in Epidermal Electronics Systems,” *ASME J. Appl. Mech.*, **81**(4), p. 044501.
- [22] Johnson, K. L., 1985, *Contact Mechanics*, Cambridge University Press, London.
- [23] Sun, J.-Y., Lu, N., Yoon, J., Oh, K.-H., Suo, Z., and Vlassak, J. J., 2011, “Inorganic Islands on a Highly Stretchable Polyimide Substrate,” *J. Mater. Res.*, **24**(11), pp. 3338–3342.
- [24] Cho, M. J., Kane, A. A., Seaward, J. R., and Hallac, R. R., 2016, “Metopic ‘Ridge’ vs. ‘Craniosynostosis’: Quantifying Severity With 3D Curvature Analysis,” *J. Cranio. Maxill. Surg.*, **44**(9), pp. 1259–1265.